Fourier–Mellin expansion coefficients of scaled pupils

Barmak Honarvar Shakibaei* **and Raveendran Paramesran**

Department of Electrical Engineering, University of Malaya, 50603 Kuala Lumpur, Malaysia

**Corresponding author: barmak.honarvar@gmail.com*

Received March 6, 2013; accepted May 13, 2013; posted online July 26, 2013

Orthogonal polynomials over the interior of a unit circle are widely used in aberration theory and in describing ocular wavefront in ophthalmic applications. In optics, Zernike polynomials (ZPs) are commonly applied for the same purpose, and scaling their expansion coefficients to arbitrary aperture sizes is a useful technique to analyze systems with different pupil sizes. By employing the orthogonal Fourier–Mellin polynomials and their properties, a new formula is established based on the same techniques used to develop the scaled pupil sizes. The description by the orthogonal Fourier–Mellin polynomials for the aberration functions is better than that by the ZPs in terms of the wavefront reconstruction errors.

OCIS codes: 010.0010, 220.0220.

doi: 10.3788/COL201311.080101.

Zernike polynomials (ZPs), which play a fundamental role in the theory of optical aberration and diffraction, have been widely used in the areas of optical testing, wavefront sensing, and ocular aberrations of human eyes[1−3]. Relating the combined aberration modes of a concentric pupil with the Zernike modes over a unit circle has been done by utilizing the ZPs[4]. ZPs have also been used in image processing theory, particularly in cases that require rotation invariant features[5−7]. Sheng *et al.* showed the difficulties in describing small images when they used ZPs for scaled-invariant imaging systems[8]. They used another set of basis functions that is orthogonal over the continuous unit circle: Fourier–Mellin polynomials (FMPs). The authors applying the new radial polynomials for image moments and showed that these polynomials had better performance than ZPs in terms of image description and noise sensitivity. Several papers have been written about the rescaling of the ZP expansion coefficients. Dai[9] showed a simple formula to scale a small-sized pupil. He derived an analytical formula to express the scaled pupil in terms of the unscaled pupil sizes. Janssen *et al.*[10] obtained a concise formula for the Zernike coefficients of scaled pupils based on the orthogonality property of ZPs. Schwiegerling[11] applied another set of basis functions called the pseudo-Zernike polynomials (PZPs). He used techniques similar to those used by Janssen *et al.* to rescale the coefficients of a related set of basis functions.

In this letter, we propose a new formula for the Fourier–Mellin coefficients of scaled pupils based on their orthogonal properties. This set of orthogonal polynomials has a relationship with the regular FMPs that are not orthogonal. FMPs are closely related to ZPs and PZPs; the only difference is on the radial polynomials between the FMPs and the ZPs or PZPs.

ZPs have been widely used as a set of basis functions because of their connection to optical systems with circular apertures. In general, ZPs are defined as

$$Z_n^m(r,\theta) = N_n^m R_n^m(r)\Theta(m\theta), \quad (1)$$

where N_n^m is the normalization factor given by

$$N_n^m = \sqrt{\frac{2(n+1)}{1+\delta_{m0}}}, \quad (2)$$

and δ_{m0} is the Kronecker delta function (i.e., δ_{m0}=1 for $m = 0$ and δ_{m0}=0 for $m \neq 0$). The radial polynomials $R_n^m(r)$ can be defined as

$$R_n^m(r) = \sum_{k=0}^{\frac{n-m}{2}} (-1)^k \frac{(n-k)!}{k!(\frac{n+m}{2}-k)!(\frac{n-m}{2}-k)!} r^{n-2k}. \quad (3)$$

The triangular function $\Theta(m\theta)$ is given by

$$\Theta(m\theta) = \begin{cases} \cos(m\theta) & m \geqslant 0 \\ -\sin(m\theta) & m < 0 \end{cases}. \quad (4)$$

The ZPs depend on a double indexing scheme where n describes the radial degree, and m describes the azimuthal frequency. The value of n is a non-negative integer, and m is an integer that satisfies $n - m =$ even.

FMPs are an alternative to ZPs, which are also orthogonal on the continuous unit circle[8]. Here, we adopted a similar definition to Eq. (1). The FMPs are defined as

$$Y_n^m(r,\theta) = N_n^m Q_n(r)\Theta(m\theta). \quad (5)$$

The normalization factor and the triangular function are identical for the two polynomial sets. The value of n is a non-negative integer, and m is an integer number. The radial polynomial of the FMPs, $Q_n(r)$, is given by

$$Q_n(r) = \sum_{s=0}^{n} \alpha_{ns} r^s, \quad (6)$$

$$\alpha_{ns} = (-1)^{n+s} \frac{(n+s+1)!}{(n-s)!s!(s+1)!}. \quad (7)$$

The presence of many factorial terms in Eq. (7) makes its computation a time-consuming task. To avoid this problem, Papakostas *et al.*[12] proposed a recursive algorithm to compute the Fourier–Mellin radial polynomials as

$$Q_n(r) = \sum_{k=0}^{n} (-1)^{n+k} T_{n,k}\, r^k,$$
$$T_{N,K} = N + 1,$$
$$T_{N,K} = \frac{(n+k+1)(n-k+1)}{k(k+1)} T_{n,k-1}\,. \quad (8)$$

The absence of the factorial terms in the aforementioned recursive method makes it superior to the direct method in Eqs. (6) and (7).

The set of polynomials $Q_n(r)$ is orthogonal over the unit disk:

$$\int_0^1 Q_n(r)\, Q_n(r) r dr = \frac{1}{2(n+1)} \delta_{nk}, \quad (9)$$

where δ_{nk} is the Kronecker symbol. This orthogonality property of the FMPs is used in deriving the pupil size scaling of the Fourier–Mellin sets. Meanwhile, the regular FMPs are not orthogonal and are defined in the ranges $r \in [0, +\infty)$ and $\theta \in [0, 2\pi]$ as

$$X_n^m(r,\theta) = r^n\, \Theta(m\theta). \quad (10)$$

Given the non-orthogonality problem of the regular Fourier–Mellin sets, the wavefront cannot be expressed in their terms. However, the radial basis orthogonal polynomials, such as the ZPs, PZPs, and FMPs, can be expressed as linear combinations of the regular Fourier–Mellin monomials.

One of the major advantages of FMPs over ZPs and PZPs is the number of zeros of the radial polynomials. The radial degree n of $Q_n(r)$ in FMPs can be significantly lower than that in ZPs and PZPs. The number of zeros of the radial polynomials corresponds to the capability of the polynomials to describe the high-spatial-frequency components of the wavefront function. For a given radial degree n and the azimuthal frequency m, the $Q_n(r)$ has n zeros, and the $R_n^m(r)$ has $(n-m)/2$ zeros. Comparing the $Q_n(r)$ and the $R_n^m(r)$ with the same number of zeros shows that the zeros of the $Q_n(r)$ are nearly uniformly distributed over the unit disc, whereas the zeros of the $R_n^m(r)$ are located in the region of large radial distance r from the origin. Figure 1 shows the distribution of the zeros of the Zernike radial and the FMPs for the same number of zeros.

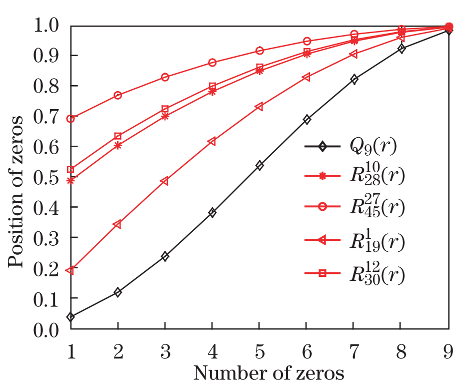

Fig. 1. Distribution of the zeros of the Zernike radial and the FMPs for the same number of zeros.

Various researchers have derived new pupil sizes based on the scaling of ZPs and PZPs[9−11]. These derivations vary in their complexity, but the final result is the same. Janssen *et al.*[10] derived a simple formula for the scaled pupils of Zernike coefficients and showed that

$$\int_0^1 R_n^m(r)\, R_k^m(\varepsilon r) r\mathrm{d}r = \frac{1}{2(n+1)} [R_k^n(\varepsilon) - R_k^{n+2}(\varepsilon)]. \quad (11)$$

In Eq. (11), let $m = 1$ and change k, n, and ε to $2k+1, 2n+1$, and $\sqrt{\varepsilon}$, respectively. The new form of Eq. (11) can be written as

$$\int_0^1 R_{2n+1}^1(r)\, R_{2k+1}^1(\sqrt{\varepsilon r}) r\mathrm{d}r = \frac{1}{4(n+1)} \left[R_{2k+1}^{2n+1}(\sqrt{\varepsilon}) - R_{2k+1}^{2n+3}(\sqrt{\varepsilon})\right]. \quad (12)$$

The radial components of the ZPs and FMPs are related by[8]

$$r\, Q_n(r^2) = R_{2n+1}^1(r). \quad (13)$$

Based on the relationship in Eq. (13), the new expression for Eq. (12) can be written as

$$\int_0^1 r Q_n(r^2) \sqrt{\varepsilon r}\, Q_k(\varepsilon\, r^2) r\mathrm{d}r = \frac{1}{4(n+1)} \left[R_{2k+1}^{2n+1}(\sqrt{\varepsilon}) - R_{2k+1}^{2n+3}(\sqrt{\varepsilon})\right]. \quad (14)$$

Changing r^2 to r in Eq. (14) results in

$$\int_0^1 Q_n(r)\, Q_k(\varepsilon r) r\mathrm{d}r = \frac{1}{2\sqrt{\varepsilon}(n+1)} \left[R_{2k+1}^{2n+1}(\sqrt{\varepsilon}) - R_{2k+1}^{2n+3}(\sqrt{\varepsilon})\right]. \quad (15)$$

Equation (15) leads to the brief description of scaling the pupil using the FMP expansions. Scaling FMPs follows an analogous procedure. If $W(r,\theta)$ is the wavefront error of an optical system, i.e., the aberrations, in the exit pupil, then it can be expanded in terms of the complete set of FMPs, $Y_n^m(r,\theta)$, with the pupil radius normalized to unity as

$$W(r,\theta) = \sum_{k=0}^{N} \sum_{m=-k}^{k} a_{km}\, Y_n^m(r,\theta), \quad (16)$$

where a_{km} is the Fourier–Mellin coefficient representing the FMP expansion into the pupil, and N is the total number of orders used for the expansion.

The goal of pupil rescaling is to derive new coefficients for the wavefront error expansion in the scaled pupils from those corresponding to the whole unit pupil. Defining a normalized scale parameter $0 \leqslant \varepsilon < 1$, the wavefront function over the new pupil is given by

$$W(\varepsilon r,\theta) = \sum_{k=0}^{N} \sum_{m=-k}^{k} b_{km}\, Y_n^m(r,\theta). \quad (17)$$

From Eq. (16),

$$W(\varepsilon r,\theta)=\sum_{k=0}^{N}\sum_{m=-k}^{k}a_{km}\,Y_n^m(\varepsilon r,\theta). \tag{18}$$

Equating Eqs. (17) and (18) and substituting Eq. (5) for the FMPs yields

$$\sum_{k=0}^{N}\sum_{m=-k}^{k}b_{km}\,N_k^m\,Q_k(r)\Theta(m\theta) =\sum_{k=0}^{N}\sum_{m=-k}^{k}a_{km}\,N_k^m\,Q_k(\varepsilon r)\Theta(m\theta). \tag{19}$$

Both sides of Eq. (19) are multiplied by $rQ_n(r)$ and integrated over r with limits of integration ranging from zero to one, giving

$$\sum_{m=-k}^{k}b_{km}\,N_k^m\left[\int_0^1 Q_n(r)\,Q_k(r)r\mathrm{d}r\right]\Theta(m\theta) =\sum_{m=-k}^{k}a_{km}\,N_k^m\left[\int_0^1 Q_n(r)\,Q_k(\varepsilon r)r\mathrm{d}r\right]\Theta(m\theta). \tag{20}$$

Using the orthogonality property of the FMPs in Eq. (9) and the obtained results in Eq. (15) leads to

$$\sum_{k=0}^{N}\sum_{m=-k}^{k}b_{km}\,N_k^m\,\delta_{nk}\,\Theta(m\theta)=\sum_{k=0}^{N}\sum_{m=-k}^{k}a_{km}\,N_k^m \times\frac{1}{\sqrt{\varepsilon}}\left[R_{2k+1}^{2n+1}(\sqrt{\varepsilon})-R_{2k+1}^{2n+3}(\sqrt{\varepsilon})\right]\Theta(m\theta). \tag{21}$$

If the triangular function is the same in both sides of Eq. (21), i.e., no rotation occurs, after the orthogonality property of the FMPs is applied, then the relationship among the new scaled pupil coefficients b_{nm} in relation to the unscaled pupil coefficients a_{nm} is expressed as

$$b_{nm}=\frac{1}{\sqrt{\varepsilon}\,N_n^m}\sum_{k=0}^{N}a_{km}\,N_k^m\left[R_{2k+1}^{2n+1}(\sqrt{\varepsilon})-R_{2k+1}^{2n+3}(\sqrt{\varepsilon})\right]. \tag{22}$$

Equation (22) describes the new scaled FMP expansion in terms of the radial components of the ZPs. Notice that $R_n^m(r)=0$ for $m>n$, and the range of the sum in Eq. (22) can be reduced from $k=n$ to N.

Meanwhile, the Schwiegerling[11] results were used to evaluate the pseudo-Zernike coefficients for the scaled pupils; these results are the same as those that we derived for the FMP expansion. Table 1 shows the coefficients b_{nm} for the scaled pupil in terms of the unit pupil using the proposed method based on the FMP expansionand the Schwiegerling method based on the PZP expansion up to the fifth order, which is the same. Using the normalized Zernike coefficients for the scaled pupils based on the similar technique[10]yields

$$b_{nm}=\frac{1}{N_n^m}\sum_{k=n}^{N}a_{km}\,N_k^m\left[R_k^n(\varepsilon)-R_k^{n+2}(\varepsilon)\right], \tag{23}$$

where $N-k$ is an even integer. Table 2 shows the coefficients of the scaled pupils based on the ZP expansion up to the fifth order.

A couple of experiments were used to validate the proposed derived formula. The first experiment compared the difference between the coefficients of the Zernike radial polynomials and those of the FMPs because the scaling factor, ε, varies between zero and one. Figure 2 shows the case of low-order coma where we scale b_{31} with $a_{31}=a_{41}=a_{51}=2\pi(0.016)$. Table 1 indicates that b_{31} for the scaled pupil using FMPs depends on all of the unscaled coefficients (a_{31},a_{41}, and a_{51}), whereas Table 2 shows that the same scaled coefficient using ZPs depend son only two unscaled coefficients (a_{31} and a_{51}).

In the second experiment, a full pupil wavefrontwas considered by the sum of the primary spherical aberration, coma, and astigmatism in terms of the radial ZPs as

$$W(r,\theta)=\sqrt{6}\,R_2^2(r)\cos(2\theta)+\sqrt{8}\,R_3^1(r)\cos(\theta)+\sqrt{5}\,R_4^0(r). \tag{24}$$

Table 1. Similar Coefficients b_{nm} for the Scaled Pupil in Terms of the Unit Pupil (Unscaled) Using FMPs (Proposed Method) and PZPs (Schwiegerling Method) up to the Fifth Order (N=5). m is a Non-negative Integer.

n	b_{nm}
0	$a_{0m}+(\varepsilon-1)\cdot\left[2\sqrt{2}\,a_{1m}+\sqrt{3}\,(5\varepsilon-3)\,a_{2m}+4\left(7\varepsilon^2-8\varepsilon+2\right)a_{3m}+\sqrt{5}\left(42\varepsilon^3-70\varepsilon^2+35\varepsilon-5\right)a_{4m}+2\sqrt{6}\left(66\varepsilon^4-144\varepsilon^3+108\varepsilon^2-32\varepsilon+3\right)a_{5m}\right]$
1	$\varepsilon\left\{a_{1m}+\sqrt{2}\,(\varepsilon-1)\left[2\sqrt{3}\,a_{2m}+2\,(7\varepsilon-5)\,a_{3m}+\sqrt{5}\left(24\varepsilon^2-32\varepsilon+10\right)a_{4m}+\frac{\sqrt{6}}{2}\left(165\varepsilon^3-315\varepsilon^2+189\varepsilon-35\right)a_{5m}\right]\right\}$
2	$\varepsilon^2\left\{a_{2m}+\frac{(\varepsilon-1)}{\sqrt{3}}\left[12\,a_{3m}+3\sqrt{5}\,(9\varepsilon-7)\,a_{4m}+2\sqrt{6}\left(55\varepsilon^2-80\varepsilon+28\right)a_{5m}\right]\right\}$
3	$\varepsilon^3\left\{a_{3m}+2\,(\varepsilon-1)\left[2\sqrt{5}a_{4m}+\sqrt{6}\,(11\varepsilon-9)\,a_{5m}\right]\right\}$
4	$\varepsilon^4\left[a_{4m}+2\sqrt{30}\,(\varepsilon-1)\,a_{5m}\right]$
5	$\varepsilon^5\,a_{5m}$

Table 2. Coefficients b_{nm} for the Scaled Pupil in Terms of the Unit Pupil (Unscaled) Using ZPs (Dai Method) up to the Fifth Order (N=5). m is a Non-negative Integer.

n	b_{nm}
0	$a_{0m}+\left(\varepsilon^2-1\right)\left[\sqrt{3}\,a_{3m}+\sqrt{5}\left(2\varepsilon^2-1\right)a_{4m}\right]$
1	$\varepsilon\left\{a_{1m}+\left(\varepsilon^2-1\right)\left[2\sqrt{2}a_{3m}+\sqrt{3}\left(5\varepsilon^2-3\right)a_{5m}\right]\right\}$
2	$\varepsilon^2\left[a_{2m}+\sqrt{15}\left(\varepsilon^2-1\right)a_{4m}\right]$
3	$\varepsilon^3\left[a_{3m}+2\sqrt{6}\left(\varepsilon^2-1\right)a_{5m}\right]$
4	$\varepsilon^4\,a_{4m}$
5	$\varepsilon^5\,a_{5m}$

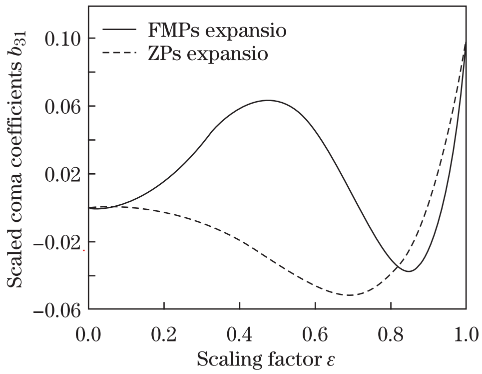

Fig. 2. Scaling lower-order coma b_{31} when $a_{31} = a_{41} = a_{51} = 2\pi(0.016)$.

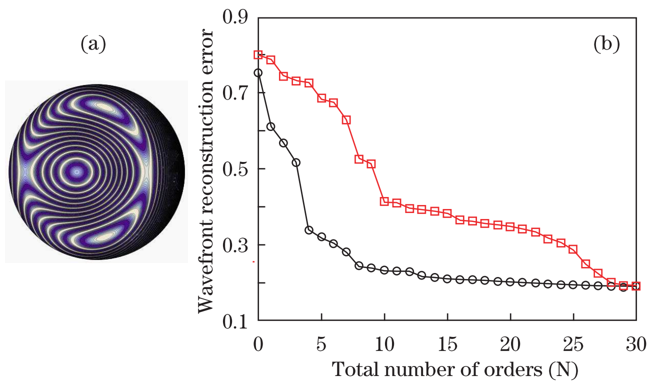

Fig. 3. (a) Wavefront contour map of the function described in Eq. (24) and (b) wavefrontreconstruction error as a function of the total number of orders.

Figure 3(a) presents the wavefront contour map of Eq. (24). The radial Zernike coefficients of the wavefront were calculated using ZPs, and the FMP coefficients of the same wavefront were calculated with Eq. (16). Figure 3(b) shows the reconstruction error of the reconstructed wavefront using ZP and FMP coefficients as a function of the total number of orders, N. In the wavefront reconstruction with FMPs, all of the radial orders $n = 0, 1, 2, \ldots, N$ were used. In the reconstruction with ZPs, all the permissible orders n satisfying the conditions $N \geqslant n$ and $N - n =$even were used. With the same total number of orders $N = 30$, the FMPs yield a considerably lower reconstruction error compared with the ZPs.

In conclusion, the proposed FMPs represent a new set of basis functions that are orthogonal over the continuous unit circle. The derived formula for the Fourier–Mellin coefficient expansion corresponding to a scaled circular pupil is equal to the formula of the pseudo-Zernike coefficient expansion derived by Schwiegerling. Finally, the radial component of the ZPs depends on both the radial degree and the azimuthal frequency, whereas the radial component of the FMPs only depends on the radial degree, which is easy to implement. Moreover, the proposed FMPs produce considerably lower wavefront reconstruction error compared with the ZPs for the same total number of orders.

This work was supported by the Engineering Faculty of the University of Malaya under Grant No. UM.C/HIR/MOHE/ENG/42.

References

1. F. Zernike, Phys. **1,** 689 (1934).
2. R. Navarro, J. Arines, and R. Rivera, Opt. Express **17,** 24269 (2009).
3. X. Pan, S. P. Veetil, C. Liu, Q. Lin, and J. Zhu, Chin. Opt. Lett. **11,** 021103 (2013).
4. S. Niu, J. Shen, W. Liao, C. Liang, and Y. Zhang, Chin. Opt. Lett. **11,** 022201 (2013).
5. A. Khotanzad, and Y. H. Hong, IEEE Trans. Pattern Anal. Mach. Intell. **12,** 489 (1990).
6. X. Gao, Q. Wang, X. LI, D. Tao, and K. Zhang, IEEE Tans. Image Process. **20,** 2738 (2011).
7. Z. Liu, Q. Li, Z. Xia, and Q. Wang, Appl. Opt. **51,** 7529 (2012).
8. Y. Sheng and L. Shen, J. Opt. Soc. Am. A **11,** 1748 (1994).
9. G.-M. Dai, J. Opt. Soc. Am. A **23,** 539 (2006).
10. A. J. E. M. Janssen and P. Dirksen, J. Micro/Nanolith. MEMS MOEMS **5,** 030501 (2006).
11. J. Schwiegerling, Opt. Lett. **36,** 3076 (2011).
12. G. A. Papakostas, Y. S. Boutalis, D. A. Karras, and B. G. Mertzios, IET Comput. Vis. **1,** 11 (2007).